IDENTIFICATION OF THE THROUGH-THICKNESS STIFFNESSES OF THICK LAMINATES BY INVERSE ANALYSIS

Fabrice PIERRON*, Sergei ZHAVORONOK**, and Michel GREDIAC***

* SMS/ Département Mécanique et Matériaux, École Nationale Supérieure des Mines de Saint-Étienne, 158, cours Fauriel, 42023 Saint-Étienne Cedex 2, France
** Moscow State Aviation Institute, Technical University
Dept. 603, 125871Volokolamskoie shosse 4, Moscow, Russia
*** LERMES, Université Blaise Pascal, 24, avenue des Landais, 63174 Aubière Cedex, France

SUMMARY: This paper presents a method to determine the four through-thickness stiffnesses of thick laminated composite rings cut from thick tubes. Only one ring specimen submitted to a diametrical compression test is required. The procedure is based on a suitable use of the principle of virtual work with four independent virtual fields. This leads to a system of four linear equations where the through-thickness stiffnesses are the unknowns. This sytem involves integrals of the strain components and the points coordinates. The system is finally inverted to determine the stiffnesses. Finite element simulations have been carried out to validate the approach and to show its stability.

KEYWORDS: thick composites, thick tubes, thick rings, diametrical compression test, stiffness measurement, identification, inverse problem, virtual fields method.

INTRODUCTION

Structural composite components in the aerospace industry are usually composed of thin plates or shells for which the knowledge of the in-plane ply moduli are enough to design the structure. However, the extension of composite applications in other industrial sectors such as the naval or ground transportation fields requires the use of less costly materials such as glass reinforced polymers, for which increased thicknesses are usually necessary to fulfil the structural function. As a consequence, the plane stress and plane strain assumption of the classical lamination theory does not hold any more and full 3D stress and strain states must be taken into account for the design. It is therefore necessary for the designer to know not only the in-plane but also the through-thickness ply moduli and strengths.

Because of the relatively new development of such structures, the measurement of through-thickness properties has seldom been addressed by researchers on composites. A number of mechanical tests are however available, ranging from direct tensile test on a through-thickness waisted or non-waisted specimen [1,2] to through-thickness shear using the Iosipescu [3] and/or the torsion test on rectangular rods and tension and/or bending on a curved specimen

[1,4]. Nevertheless, the reliability of these methods is often questionable mainly because of the difficulty to achieve homogeneous stress states in the specimens.
The aim of this paper is to describe an alternative method allowing the determination of the through-thickness stiffnesses from a testing configuration giving rise to heterogeneous stress fields inside the specimen. The geometry is a thick composite ring cut in a thick composite tube. Such structures are very important for offshore applications [5] and usual methods such as the Iosipescu test or the direct tension test cannot be used to characterize them. The specimen is subjected to diametral compression. This testing configuration can be easily setup in practice using a universal tension/compression testing machine. Through-thickness stresses occur inside the specimen and it is shown below that the corresponding stiffnesses can be determined with a suitable identification procedure.
The main features of the method described in the present paper are the following ones:
- heterogeneous strain fields such that the whole set of unknown parameters is involved in the specimen response are considered and processed;
- the magnitude of the applied load as well as the whole displacement or strain fields are considered as input data;
- no analytical solution is required *a priori*;
- the unknown parameters are determined directly, without any iterative calculations.

It must be pointed out that most of the similar procedures available in the literature are based on mixed experimental/numerical approaches: the response of the tested specimen is modelled with a finite element programme or with another approximated procedure like the Ritz method and the unknown parameters are adjusted stepwise, in such a way that both sets of measured and computed values of the displacements, strains or natural frequencies match as precisely as possible (see for instance Refs. 6-10]). Initial values close to the actual ones are often required to obtain the convergence of the process. These drawbacks are presently avoided as the stiffnesses are determined directly.
The theoretical aspects of the procedure are described in the first part of the paper. Some results of finite element simulations are then given for a specific specimen geometry. The stability of the procedure is finally examined.

THEORY

Introduction

The method used herein is based on a relevant use of the principle of virtual work. It has been introduced first by Grédiac [11] for anisotropic plate bending problems, both in statics [12] and in dynamics [13] and for in-plane problems [14]. The whole strain field is required for such a method. It can be obtained in practice with an optical method [15], but this point is not developed here. The basic idea is to apply the principle of virtual work to the tested specimen with some explicit and independent virtual displacement fields. Each new virtual field provides a new linear equation where the stiffnesses are unknown. This leads to a linear system which has to be inverted. This method is very general but two main difficulties arise in practice. First, one has to define a specimen geometry where the influences of each unknown are approximately balanced to ensure its “identifiability”. Second, a set of admissible virtual fields leading to a well-conditioned system must be found. This will be solved in the following sections in the case of the determination of the through-thickness stiffnesses.

Principle of virtual work with specific virtual fields

An orthotropic medium characterised by four independent stiffnesses is considered. Because of the shape of the specimen studied below, polar coordinates are used. In this coordinate system and assuming a linear elastic behaviour, the independent stiffnesses to be identified relate the in-plane stress to the strain components as follows

$$\begin{pmatrix} \sigma_r \\ \sigma_\theta \\ \sigma_s \end{pmatrix} = \begin{bmatrix} Q_{rr} & Q_{r\theta} & 0 \\ Q_{r\theta} & Q_{\theta\theta} & 0 \\ 0 & 0 & Q_{ss} \end{bmatrix} \begin{pmatrix} \varepsilon_r \\ \varepsilon_\theta \\ \varepsilon_s \end{pmatrix} \tag{1}$$

where σ_i and ε_i with i,j=r,θ,s are the components of the stress and strain tensors respectively (the classical contraction from 2 to 1 for the stress and strain indices is used), the Q_{ij}'s are the stiffnesses to be determined.
The present identification method is based on the principle of virtual work which can be written in the following form

$$-\int_V \sigma_{ij}\varepsilon^*_{ij}dV + \int_{\partial V} T_i u^*_i dS = 0 \tag{2}$$

where the convention of repeated indices for summation is adopted, V is the volume of the specimen considered, ∂V its boundary, σ the stress tensor, ε^* the virtual strain tensor, T the surface load density, u^* the virtual displacement field associated to ε^*. The first term is the internal virtual work and the second one is the external virtual work. Considering now that the problem is an in-plane one and that the specimen is subjected to a force P applied at a point M, equation (2) becomes

$$\int_S \sigma_r\varepsilon^*_r dS + \int_S \sigma_\theta\varepsilon^*_\theta dS + \int_S \sigma_s\varepsilon^*_s dS = \frac{Pu^*(M)}{e} \tag{3}$$

where e is the thickness of the specimen, S its surface, $u^*(M)$ the virtual displacement along the direction of the loading and P the magnitude of the load (P>0).
Introducing now equation (1) in equation (3) and assuming that the material properties are homogeneous over the specimen

$$Q_{rr}\int_S \varepsilon_r\varepsilon^*_r dS + Q_{\theta\theta}\int_S \varepsilon_\theta\varepsilon^*_\theta dS + Q_{r\theta}\int_S (\varepsilon_r\varepsilon^*_\theta + \varepsilon_\theta\varepsilon^*_r)dS + Q_{ss}\int_S \varepsilon_s\varepsilon^*_s dS = \frac{Pu^*(M)}{e} \tag{4}$$

As may be seen, a linear equation involving the four unknown stiffnesses is obtained. The objective is now to define the shape of the specimen and at least four independent virtual fields to build up a linear system where the stiffnesses are unknown.

Shape of the tested specimen

The choice of the specimen shape as well as of the loading conditions is somewhat arbitrary, but it must follow some obvious rules. For instance, the specimen must be easily manufactured and the magnitude of the three in-plane stress components inside the loaded specimen must be approximately balanced to ensure the “identifiability” of the stiffnesses.

The geometry studied here is a thick ring obtained for instance from a thick composite tube (see Fig. 1).

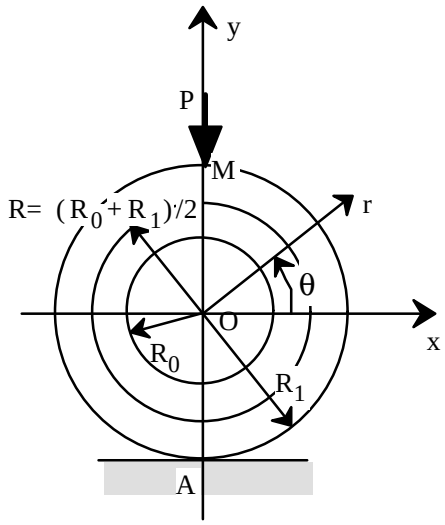

Fig. 1: Schematic view of the ring compression test specimen

It is subjected to a unique radial force. The first point is to check that these loading conditions are relevant: *i.e.* that the magnitude of the three stress components are roughly the same. Hence, a finite element calculation has been carried out with the following material properties:

$$E_{\theta\theta} = 40\ \text{GPa}\ , E_{rr} = 10\ \text{GPa}\ , G_{r\theta} = 4\text{GPa}\ , \nu_{\theta r} = 0.3 \tag{5}$$

These quantities are directly related to the unknown stiffnesses

$$E_{rr} = Q_{rr}\left(1 - \frac{Q_{r\theta}^2}{Q_{rr}Q_{\theta\theta}}\right),\ E_{\theta\theta} = Q_{\theta\theta}\left(1 - \frac{Q_{r\theta}^2}{Q_{rr}Q_{\theta\theta}}\right),\ \nu_{\theta r} = \frac{Q_{r\theta}}{Q_{\theta\theta}},\ G_{r\theta} = Q_{ss} \tag{6}$$

The model has been developed with the ANSYS 5.3. package. The following dimensions of this specimen have been used (see Fig. 1):

$$R_1 = 87.5\,\text{mm}\ ; R_0 = 37.5\,\text{mm}\ , R = 62.5\,\text{mm}\ , h = 50\ \text{mm}\ , e = 50\,\text{mm} \tag{7}$$

Because of the symmetry of the problem, only one quarter of ring has been considered and meshed with 1500 bilinear elements (plane42): 30 along the width and 50 along the quarter of the circle. It has been checked with a convergence study that the results provided by the programme are satisfactory. It was thus verified that the three stress components are of roughly equal magnitudes, which confirms the potential "identifiability" of the four stiffness components in this case.

Virtual fields used for the identification procedure

Introduction

The problem is now to define four different virtual fields. Note that more than four fields could be used to obtain a redundant system, but this approach has not been retained in the present work. The virtual fields have only to be continuous and kinematically admissible. Hence, a

wide range of choices is available for these fields, which will be defined following the general rules listed below:

- *i)* the four fields must be independent to ensure the independence of the equations;
- *ii)* previous investigations carried out with a similar approach have shown that the literal expression of the fields must be as simple as possible to ensure the stability and the accuracy of the procedure;
- *iii)* to improve the independence of the equations, the fields must lead to partially uncoupled equations, i.e. only some of the unknowns must appear in the equations if possible. Ideally, the best choice should lead to an internal work in which only one stiffness is involved, but this it is not always possible to achieve;
- *iv)* depending on the specimen geometry, either the whole surface of the specimen or only one particular part can be virtually deformed. In both cases however, the area where the virtual strain components are maximum must match as much as possible the area where the actual stress components are maximum to reduce the influence of measurement errors on the actual strain on the internal virtual work.

In conclusion, virtual fields can be considered as filters which emphasize the contribution of some of the unknowns or some of the parts of the specimen to the internal virtual work. This feature is used to define the testing configurations and to choose the virtual fields.

Virtual fields

The choice of the proposed fields is more or less intuitive and somewhat arbitrary, but it is checked that they follow the above rules as much as possible and that they lead in practice to the unknown stiffnesses. Each of the following fields are of the form

$$\vec{u}^* = u_r^* \vec{e}_r + u_\theta^* \vec{e}_\theta + K \vec{e}_y \tag{8}$$

where u_r^*, u_θ^* are the virtual displacements in the natural polar coordinate system (O,r,θ) of the specimen (see Fig. 1), $\vec{e}_r$, $\vec{e}_\theta$ and $\vec{e}_y$ are normalized vectors along the r-, θ- and y- axes respectively. $K\vec{e}_y$ is a constant global displacement that is adjusted in such a way that point A located at the bottom of the ring does not move. Hence, the virtual displacement field is admissible. Note that this constant term has no influence on the virtual strain field as it vanishes after differentiation.

<u>- Field 1</u>: virtual hydrostatical compression

The first field can be considered as a virtual hytrostatical compression. It is defined by

$$u_r^* = -kr, u_\theta^* = 0, K = -kR_1 \tag{9}$$

where k and K are any non-zero real numbers. The virtual strain components are obtained by differentiation of the virtual displacement field using the following relationship in a given polar coordinate system

$$\varepsilon_r = \frac{\partial u_r}{\partial r}, \varepsilon_\theta = \frac{1}{r}\frac{\partial u_\theta}{\partial \theta} + \frac{u_r}{r}, \varepsilon_s = \frac{\partial u_\theta}{\partial r} + \frac{1}{r}\frac{\partial u_r}{\partial \theta} - \frac{u_\theta}{r} \tag{10}$$

In the present case, the virtual strain components are

$$\varepsilon_r^* = \varepsilon_\theta^* = -k, \varepsilon_s^* = 0 \tag{11}$$

The virtual displacement of point M is

$$\vec{u}^*(M) = -2kR_1\vec{e}_y \tag{12}$$

Finally, equation (4) becomes

$$Q_{rr}\int_0^{2\pi}\int_{R_0}^{R_1}\varepsilon_r r dr d\theta + Q_{r\theta}\int_0^{2\pi}\int_{R_0}^{R_1}(\varepsilon_r + \varepsilon_\theta) r dr d\theta + Q_{\theta\theta}\int_0^{2\pi}\int_{R_0}^{R_1}\varepsilon_\theta r dr d\theta = \frac{2PR_1}{e} \tag{13}$$

<u>- Field 2</u>: virtual bending

The second field describes a virtual bending of the circle. It is built under the Euler-Bernoulli's assumption to eliminate the contribution of Q_{rr} and Q_{ss}. Virtual displacements can be expressed as follows in the natural polar coordinate system

$$u_r^* = kr\cos 2\theta, u_\theta^* = 2k(r-R)\sin 2\theta, K = -kR \tag{14}$$

In this case, equation (5) becomes

$$Q_{r\theta}\int_0^{2\pi}\int_{R_0}^{R_1}\varepsilon_r\left(r - \frac{3}{4}R\right)\cos 2\theta dr d\theta + Q_{\theta\theta}\int_0^{2\pi}\int_{R_0}^{R_1}\varepsilon_\theta\left(r - \frac{3}{4}R\right)\cos 2\theta dr d\theta = \frac{PR}{2e} \tag{15}$$

<u>- Field 3</u>: virtual shear

The third field is such that only the shear strain is non-zero, so that only the shear modulus is involved in the internal virtual work. In the natural coordinate system, the virtual displacement field is

$$u_r^* = kR\cos 2\theta, u_\theta^* = -\frac{k}{2}R\sin 2\theta, K = -kR \tag{16}$$

Equation (5) reduces to

$$Q_{ss}\int_0^{2\pi}\int_{R_0}^{R_1}\varepsilon_s \sin 2\theta dr d\theta = \frac{4P}{3e} \tag{17}$$

<u>- Field 4</u>: virtual swelling

The fourth field describes a swelling of the circle. In the natural polar coordinate system, the virtual displacement field is

$$u_r^* = k(r-R)\cos 2\theta, u_\theta^* = 0, K = -\frac{kh}{2} \tag{18}$$

As a result, the four unknowns are related to the load applied to the ring

$$Q_{rr}\int_0^{2\pi}\int_{R_0}^{R_1}\varepsilon_r r\cos 2\theta dr d\theta + Q_{r\theta}\left[\int_0^{2\pi}\int_{R_0}^{R_1}\varepsilon_r(r-R)\cos 2\theta dr d\theta + \int_0^{2\pi}\int_{R_0}^{R_1}\varepsilon_\theta r\cos 2\theta dr d\theta\right] +$$
$$Q_{\theta\theta}\int_0^{2\pi}\int_{R_0}^{R_1}\varepsilon_\theta(r-R)\cos 2\theta dr d\theta - 2Q_{ss}\int_0^{2\pi}\int_{R_0}^{R_1}\varepsilon_s(r-R)\sin 2\theta dr d\theta = \frac{Ph}{e} \tag{19}$$

The detailed calculations can be found in Ref. [17].

Conclusion

It has been shown that the application of the principle of virtual work with four independent virtual fields leads to a system of four partially uncoupled linear equations where the stiffnesses are unknown. This system can be written as follows

$$\mathbf{Aq} = \mathbf{b} \quad \boxed{\mathbf{Aq}=\mathbf{b}} \tag{20}$$

where **q** is the unknown vector

$$\mathbf{q}:\{Q_{ss}, Q_{rr}, Q_{r\theta}, Q_\theta\}^t \tag{21}$$

A is the 4x4 matrix of the linear system:

$$\mathbf{A}:\begin{bmatrix} 0 & A_{12} & A_{13} & A_{14} \\ 0 & 0 & A_{23} & A_{24} \\ A_{31} & 0 & 0 & 0 \\ A_{41} & A_{42} & A_{43} & A_{44} \end{bmatrix} \tag{22}$$

with

$$A_{12} = \int_0^{2\pi}\int_{R_0}^{R_1}\varepsilon_r r dr d\theta, A_{13} = \int_0^{2\pi}\int_{R_0}^{R_1}(\varepsilon_r+\varepsilon_\theta) r dr d\theta, A_{14} = \int_0^{2\pi}\int_{R_0}^{R_1}\varepsilon_\theta r dr d\theta$$
$$A_{23} = \int_0^{2\pi}\int_{R_0}^{R_1}\varepsilon_r\left(r-\frac{3}{4}R\right)\cos 2\theta dr d\theta, A_{24} = \int_0^{2\pi}\int_{R_0}^{R_1}\varepsilon_\theta\left(r-\frac{3}{4}R\right)\cos 2\theta dr d\theta$$
$$A_{31} = \int_0^{2\pi}\int_{R_0}^{R_1}\varepsilon_s\sin 2\theta dr d\theta \tag{23}$$
$$A_{41} = -2\int_0^{2\pi}\int_{R_0}^{R_1}\varepsilon_s(r-R)\sin 2\theta dr d\theta, A_{42} = \int_0^{2\pi}\int_{R_0}^{R_1}\varepsilon_r r\cos 2\theta dr d\theta,$$
$$A_{43} = \int_0^{2\pi}\int_{R_0}^{R_1}[\varepsilon_r(r-R)+\varepsilon_\theta r]\cos 2\theta dr d\theta, A_{44} = \int_0^{2\pi}\int_{R_0}^{R_1}\varepsilon_\theta(r-R)\cos 2\theta dr d\theta$$

and **b** is the right hand side vector:

$$\mathbf{b}: P.\left\{\frac{2R_1}{e}, \frac{R}{2e}, \frac{4}{3e}, \frac{h}{e}\right\}^t \tag{24}$$

As may be seen, two equations are partially uncoupled and one is completely uncoupled. This result illustrates the above rule *iii)*.
A system of four linear equations has been built up. The purpose of the next section is to validate the present approach using some finite element simulations. Strain fields provided by the finite element model of the specimen are considered as input data to compute the integrals in matrix **A**. Stiffness components are finally back-identified and compared to the input values of the finite element model to assess the accuracy and the stability of the procedure.

NUMERICAL SIMULATIONS

Identification

The output data of the finite element calculation described previously in terms of strains at the centroid of each element are considered as input data for the identification programme.
The integrals of the strain components in matrix **A** are transformed into discretized sums (see Ref. [17]). The linear system is solved in order to identify the stiffness components E_{rr}, $E_{\theta\theta}$, $\nu_{\theta r}$ and $G_{r\theta}$. The magnitude of the applied load P is 200 000 N. The results are reported in Table 1. As can be seen, the identified values agree within less than 1% to the reference values. This results validates the procedure from a theoretical point of view.

Table 1: Actual and identified values of the stiffness components

	$E_{\theta\theta}$ *GPa*	E_{rr} *GPa*	$G_{r\theta}$ *GPa*	$\nu_{\theta r}$ -
Actual value	40.00	10.00	4.00	0.30
Identified value	40.16	9.97	4.00	0.297
Relative difference %	0.4	-0.3	0.0	-1.0

Stability

As the present identification method will be used in experimental applications, it is important to check its stability as the strain components cannot be exactly collected in practice. Therefore, experimental errors have been numerically simulated by adding noise to the strain components. This noise is modelled with a truncated normal distribution of errors supposed to simulate experimental errors. Two magnitudes have been chosen, 5% and 10% of the maximum strain component for each of three strain components. The standard deviation of the error distribution is also computed. These perturbated data are considered as input data for the identification programme and the corresponding identified stiffnesses are collected. The process is repeated 50 times to obtain a distribution of perturbated identified stiffnesses. To check the stability, the amplitude and mean of these identified distributions have been compared to the original input stiffnesses and to the perturbation amplitude. The calculations have been performed for both amplitudes of errors. The coefficient of variation, which is defined by the ratio between the standard deviation and the mean, is also computed in each case. This quantity is directly related to the scatter of the distribution. The results are reported

in Tables 2. It can be seen that the difference between the mean value of the identified moduli computed from the perturbated strain components and the actual corresponding quantities is lower than 1.7%. Poisson's ratio is obtained with a relative difference of 10% in the second case. This last result is in agreement with the conclusions of previous studies carried out on other specimen shapes and loading conditions, in which it was shown that the lowest accuracy is obtained with Poisson's ratio because of its small influence on the strain and stress fields. It must be emphasized that the coefficients of variation remain reasonably low for E_{rr}, $E_{\theta\theta}$ and $G_{r\theta}$, even for the 10% perturbation. This is due to the fact that the integrals can be interpreted as weighted means of the strain components that average out local variations.

Table 2: Identified stiffness distributions from 5% perturbated strains

	$E_{\theta\theta}$ *GPa*	E_{rr} *GPa*	$G_{r\theta}$ *GPa*	$\nu_{\theta r}$ -
Actual values	40.00	10.00	4.00	0.30
Perturbated values	40.36	9.88	4.00	0.29
Relative difference (%)	0.9	-1.2	0.0	-2.7
Coefficient of variation (%)	4.8	5.2	0.3	20.3

Table 3: Identified stiffness distributions from 10% perturbated strains

	$E_{\theta\theta}$ *GPa*	E_{rr} *GPa*	$G_{r\theta}$ *GPa*	$\nu_{\theta r}$ -
Reference values	40.00	10.00	4.00	0.30
Perturbated values	40.37	9.82	4.00	0.27
Relative difference (%)	0.9	-1.7	-0.0	-10.0
Coefficient of variation (%)	12.0	13.1	0.8	60.8

CONCLUSION

An identification method has been proposed for determining the through-thickness stiffnesses of thick laminated composites. These properties are difficult to measure with standard methods and such alternative approaches can therefore be considered advantageously.
The main features of the present method are :

- heterogeneous stress and strain fields are considered and processed ;
- no assumption is made concerning the displacement field ;
- the whole strain field is considered as input data of the identification procedure ;
- only one test is required to determine the four independent parameters ;
- the method itself is based on a relevant use of the principle of virtual work with four independent fields ;
- the method is direct and neither finite element model nor iterative calculations are required ;
- the accuracy and the stability of the procedure have been studied and the results can be considered as compatible with a practical application.

One could think that the main difficulty lies in the whole strain field measurement that is performed in practice with a suitable optical method. However, such setups become now more and more popular, reliable and unexpensive. Previous similar studies on other specimen shapes

and loading conditions for measuring in-plane and bending stiffnesses of thin composite have been successfully carried out with grid techniques or deflectometry setups [15,16]. As a result, one can expect to actually measure the through-thickness stiffnesses with the present approach.

REFERENCES

1. Broughton, W.R. and Sims, G.D., "An overview of through-thickness test methods for polymer matrix composites", *NPL report DMM(A) 148*, National Physical Laboratory, UK, 1994.
2. Mespoulet, S., "Through-thickness test methods for laminated composite materials", Ph.D Thesis, Imperial College of Science, Technology and Medicine, 1998.
3. Gipple, K.L. and Hoyns, D., "Measurement of the out-of-plane shear response of thick section composite materials using the V-notched beam specimen", *Journal of Composite Materials*, Vol. 28, No. 6, 1994, pp. 543-572.
4. Hiel, C., Surnish, M. and Chappell, D., "A curved beam specimen for determining the interlaminar tensile strength of a laminated composite", *Journal of Composite Materials*, Vol. 25, 1991, pp. 854-868.
5. Pierron, F. and Davies, P., "Ring compression test for cylindrical composite mechanical characterization", *Proceedings of the CTS4 conference* (Composite Testing and Standardization), 31 August-2 September 1998 in Lisbon, Portugal, pp. 193-202.
6. Sol, H., "Identification of anisotropic plates rigidities using free vibration data", PhD. Thesis, Free University of Brussels, 1986.
7. Hendriks, M.A.N., "Identification of the mechanical properties of solid materials", PhD. Thesis, Eindhoven University of Technology, 1991.
8. De Wilde, W.P., "Identification of the rigidities of composite systems by mixed numerical/experimental methods", *Mechanical identification of composites*. Elsevier, Amsterdam, 1991, pp. 1-15.
9. Mota Soares, C.M., Moreira de Freitas, M., Araujo, A. L. and Pedersen, P., "Identification of material properties of composite plate specimens", *Composite Structures*, Vol. 25, 1993, pp. 277-285.
10. Frederiksen, P.S., "Experimental procedure and results for the identification of elastic constants of thick orthotropic plates", *Journal of Composite Materials*, Vol. 31, No. 4, 1997, pp. 360-382.
11. Grédiac, M., "Principe des travaux virtuels et identification/Principle of virtual work and identification", Comptes rendus de l'Académie des Sciences. II/309, 1989, pp. 1-5, in French with abridged English version.
12. Grédiac, M., "On the direct determination of invariant parameters governing the bending of anisotropic plates", *International Journal of Solids and Structures*., Vol. 33, No. 27, 1996, pp. 3969-3982.
13. Grédiac, M., Fournier, N., Paris, P.-A. and Surrel, Y., "Direct identification of elastic constants of anisotropic plates by modal analysis : experiments and results", *Journal of Sound and Vibration*, Vol. 210, No. 5, 1998, pp. 645-659.
14. Grédiac, M. and Pierron, F., "A T-shaped specimen for the direct characterization of orthotropic materials", *International Journal for Numerical Methods in Engineering*, Vol. 41, 1998, pp. 293-309.
15. Grédiac, M., Fournier, N., Paris, P.-A. and Surrel, Y., "Direct measurement of invariant parameters of composite plates", *Journal of Composite Materials*, Accepted for publication, 1998.
16. Grédiac, M., Pierron, F. and Surrel, Y., "Novel procedure for complete in-plane composite characterization using a T-shaped specimen", *Experimental Mechanics*, Accepted for publication, 1998.

17. Pierron, F., Zhavoronok, S. and Grédiac, M., "Identification of the through-thickness properties of thick laminates using the virtual fields method", *International Journal of Solids and Structures*, 1998, submitted.